Implant-Prosthodontic Discrepancy of Complete-Arch Cobalt-Chromium Implant Frameworks Manufactured Through Selective Laser Melting Additive Manufacturing Technology Using a Coordinate Measuring Machine

Marta Revilla-León, DDS, MSD[1]/Laura Ceballos, DDS, PhD[2]/Mutlu Özcan, DDS, Dr Med Dent, PhD[3]

Purpose: *The objective was to measure the implant-prosthodontic discrepancy of complete-arch implant-supported frameworks made of cobalt-chromium (Co-Cr) fabricated using selective laser melting (SLM) additive manufacturing technologies.* ***Materials and Methods:*** *A completely edentulous maxillary cast with seven implant replicas was obtained. Co-Cr SLM frameworks (n = 9) from three different providers (SLM-1, SLM-2, SLM-3) were manufactured. A coordinate measuring machine was selected to measure the implant-prosthodontic discrepancy (μm) on the x-, y-, and z-axes and the 3D gap (3D = $\sqrt{x^2 + y^2 + z^2}$ where implants were considered as the statistical unit (n = 7). One-way analysis of variance (ANOVA), Student-Newman-Keuls, and Tukey tests were used to analyze the data (α = .05).* ***Results:*** *The mean 3D implant-prosthodontic discrepancy (μm) was higher for SLM-1 (73.77 ± 27.94) than for SLM-2 (47.54 ± 22.63) and SLM-3 (47.26 ± 22.57). At the x-axis, SLM-2 showed a significantly smaller gap (16.21 ± 9.6) than SLM-3 (32.92 ± 27.77) and SLM-1 (34.77 ± 21.85). At the y-axis, however, SLM-3 presented a significantly smaller gap (27.97 ± 9.49) than SLM-2 (38.84 ± 27.82) and SLM-1 (54.35 ± 29.89). Similarly, at the z-axis, SLM-3 (4.01 ± 2.29) showed the least gap, followed by SLM-2 (9.09 ± 7.63), which was significantly smaller than that of SLM-1 (16.14 ± 21.09).* ***Conclusion:*** *The three SLM additive manufacturing technologies tested showed implant-prosthodontic discrepancies ranging from 4.01 to 54.35 μm, which could be considered in the clinically acceptable range. Distortion at the z-axis was significantly less compared with the x- and y-axes in all the groups tested.* Int J Oral Maxillofac Implants 2019;34:698–707. doi: 10.11607/jomi.6739

Keywords: *3D printing, additive manufacturing technologies, chrome-cobalt, implant-prosthodontic gap, selective laser melting*

Computer-aided design/computer-aided manufacturing (CAD/CAM) technologies involve the processes where the design and fabrication of a prosthesis is guided by computers. This digital workflow contains three main phases, namely, digitizing procedures, data processing, and manufacturing methodologies.[1]

Data acquisition contains the procedures in which a three-dimensional (3D) model is obtained through digitizing tools, such as intraoral or extraoral scanning devices.[2,3] In the data processing step, the obtained data are represented by a point cloud that uses mathematical algorithm calculations, the aberrant points are removed, and the density of the point cloud information is optimized.[3,4] This triangulation method obtains a mesh, which is then interpreted as a 3D model of the digitized object by CAD software, and used to design a prosthesis. Once this CAD design is accomplished, a standard tessellation language (STL) file is attained.[5] Lastly, the virtual design of the framework for an implant-supported prosthesis is manufactured through additive or subtractive methodologies.

Additive manufacturing has been defined as "a process of joining materials to make objects from 3D model data, usually layer upon layer".[6] The American Society for Testing and Materials (ASTM) has

[1]Assistant Professor and Assistant Program Director, AEGD Residency, College of Dentistry, Texas A&M University, Dallas, Texas, USA; Affiliate Faculty Graduate Prosthodontics, University of Washington, Seattle, Washington, USA; Researcher, Revilla Research Center, Madrid, Spain.
[2]Associate Professor, Area of Stomatology, Rey Juan Carlos University, Madrid, Spain.
[3]Professor, Head of Dental Materials Unit, Clinic for Fixed and Removable Prosthodontics and Dental Materials Science, Center for Dental and Oral Medicine, University of Zurich, Zurich, Switzerland.

Correspondence to: Dr Marta Revilla-León, 3302 Gaston Avenue, Room 713, Dallas, TX 75246, USA.
Email: revillaleon@tamhsc.edu

Submitted November 3, 2017; accepted January 22, 2019.

determined seven additive families: material jetting, stereolithography, material extrusion, powder bed fusion (PBF), sheet lamination, binder jetting, and direct energy deposition.[5] The technologies employed to additively manufacture dental metal prostheses are the PBF technologies,[2] namely, selective laser sintering (SLS), selective laser melting (SLM), and electron beam melting (EBM).[6,7]

PBF technologies employ a laser (fiber lasers, Nd:YAG lasers) or electron beam focused to fuse thin layers (20 to 100 μm) from a bed of powdered metal until the 3D object is completely built (Fig 1).[8–10] With the SLS technology, the laser energy heats and consolidates metal powder layer upon layer.[10–12] Normally, the SLS additive manufacturing has obtained sintered objects, but they are strong enough to be used for many applications.[13–17] However, the SLM and EBM technologies have the capability to completely melt the metal powder compared with the SLS technology.[6,18–21] There are several characteristics that differentiate between the PBF technologies, namely, the energy source (fiber lasers, Nd:YAG lasers, or electron beam),[21–24] temperature reached,[20,23,24] chamber condition (argon, nitrogen, or helium),[20,23,24] energy power (100 to 500 W to 7 kW),[20,23,24] grain size (20 to 105 mm),[24,25] and layer thickness (10 to 50 mm).[24,25]

Previous studies have evaluated the mechanical properties of the additive manufacturing metals obtained through PBF procedures.[24–31] Those studies concluded that the additive manufacturing metal could obtain better mechanical properties than those metals obtained using the conventional casting procedures.[24–31] Moreover, some studies concluded that additive manufacturing metal can provide similar or slightly improved mechanical properties compared with the metal obtained through subtractive methods.[24–31]

The characteristic superficial texture of the layer-by-layer buildup in additive manufacturing technologies would result in a rough metal surface. A strong correlation has been reported between the roughness values on the mating surfaces and the implant-prosthodontic discrepancy.[32] In order to achieve acceptable implant-prosthodontic discrepancy, the manufacturers have combined PBF additive manufacturing technologies and subtractive methods. The metal framework is fabricated using PBF additive manufacturing technologies overcontouring the implant interface, and, posteriorly, the implant interface is shaped using milling technology. These technology combinations involve an accurate process translating the metal framework from the 3D printer to the milling machine.[33]

There are only a few studies reporting on the implant-prosthodontic discrepancy using combined additive and subtractive technologies.[32,33] A previous study[33] analyzed the implant-prosthodontic discrepancy of complete-arch titanium (Ti6Al4V) implant-supported frameworks fabricated with two additive manufacturing technologies: SLM and EBM procedures using a coordinate measuring machine (CMM). The results showed no significant differences between the SLM and EBM additive manufacturing technologies. The mean 3D discrepancy was reported as 67 ± 13.5 mm for the SLM additive manufacturing process and 60.2 ± 18.5 mm for the EBM additive manufacturing fabrication method, both of which were considered clinically acceptable values.

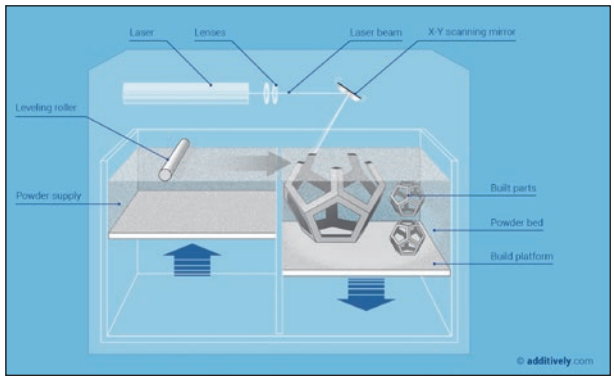

Fig 1 Illustration of selective laser melting (SLM) technology working mechanism. Reprinted from Additevely.com with permission.

Similar to the conventional fixed prosthodontics, with the CAD/CAM workflow, implant-supported framework discrepancy is usually influenced by multiple factors,[32–36] such as implant position, depth, angulation and distance between the implants, the impression technique and material used, digitalization techniques of the definitive cast, design of the framework, manufacturing process, experience of the dental technician, or the machining tolerance of the prosthetic abutments.[37–41]

Adequate implant-prosthodontic discrepancy was described as passive fit at a level that did not produce any long-term clinical complications where discrepancies less than 150 μm were considered adequate.[41] Previous authors have proposed that the framework discrepancy was clinically unacceptable when more than half-a-turn was required in order to tighten the screw completely after its initial seating resistance was encountered.[42] Even though those recommended parameters have an empirical origin, they are used as a reference to define the clinically acceptable implant-prosthodontic discrepancy thresholds.[41]

A CMM examination is extensively selected in implant dentistry to evaluate the implant-prosthodontic discrepancy on the x-, y-, and z-axes.[43–45] Previous studies showed that the implant-prosthodontic misfit of the

Fig 2 Maxillary definitive conventional stone cast with seven implant replicas of a patient.

frameworks is present either produced by conventional casting procedures or computer numerical control (CNC) machining.[25–29] The range of the gap is different depending on the implant design of the connection,[26] the number of units of the frameworks,[25–28] and the x-, y-, and z-axes evaluated.[25–31,42] It is, however, unclear whether or not these PBF additive manufacturing technologies in combination with CNC procedures generate frameworks with acceptable accuracies.

The goal of the present study was to measure the implant-prosthodontic discrepancy of complete-arch implant-supported frameworks made of Co-Cr manufactured through SLM additive manufacturing technology from three different providers using a CMM machine. The null hypothesis was established: there would be no significant difference on the mean implant-prosthodontic discrepancy values between the different SLM additive manufacturing providers on the x-, y-, and z-axes and 3D gap calculations.

MATERIALS AND METHODS

Specimen Fabrication

One edentulous maxillary definitive stone cast with implant replicas (n = 7) (Tissue Level RN Straumann Implant replicas, Straumann) and the duplicated maxillary screw-retained interim restoration (nonreflective acrylic resin, Palapress Vario, Heraeus-Kulzer) of a patient were obtained (Fig 2).

A tactile (Renishaw DS10 Scanner, Renishaw) and optical (Renishaw DS20, Renishaw) scanner with specific dental CAD software (Exocad Dental CAD 2.1, Exocad) were used to digitize the maxillary master cast and duplicated provisional restorations. The dental CAD software was employed for the virtual design of the maxillary complete-arch implant-supported framework. When the design was completed, the STL_1 file was obtained.

The STL_1 file was used to manufacture all the metal frameworks, using three different SLM additive manufacturing systems (Tables 1 and 2 and Figs 3a to 3d). A total of 9 additive manufacturing metal frameworks were manufactured (n = 3 frameworks per group), with a total of 56 implants (Figs 4a to 4c).

Measurements

A CMM (Zeiss Contura, Carl Zeiss Industrielle Messtechnik) was used to analyze the implant-prosthodontic discrepancy by an independent laboratory (Fig 5). The implant analog positions of the master cast were measured and used as a reference for implant-prosthodontic discrepancy assessment with the 9 different frameworks for each implant replica.[45]

The master cast and the additive manufacturing metal frameworks were placed in a mold seated on a reinforced-concrete table. A 0.5-mm tactile stylus under 0.1-N pressure was used to calculate the center point of each of the implant analogs of the master cast in the three dimensions by calculating different points on the most coronal part of each implant analog by mapping the x-, y-, and z-axes. The same procedure was repeated within the intaglio surface of each implant interface in all the additive manufacturing metal frameworks specimens. These data were used to analyze the 3D x-, y-, and z-axes discrepancy between the implant analogs of the master cast and each additive manufacturing metal framework with the least square best-fit technique[46,47] using specific software (Geomagic, 3D Systems). The 3D gap distortion was calculated using the formula $3D = \sqrt{x^2 + y^2 + z^2}$. Each measurement was repeated three times. All the measurements were performed by the same experienced operator.

Statistical Analysis

Statistical analysis was performed using specific software (SPSS 19.0 for Windows, IBM Corporation). Mean values and standard deviations per group were analyzed. The homogeneity of the data was evaluated using the Kolmogorov-Smirnov test. The data (implant-prosthodontic gap [µm] in x-, y-, and z-axes and 3D gap) were submitted to one-way analysis of variance (ANOVA) with repeated measures. Multiple comparisons were made using Student-Newman-Keuls and Tukey's tests. *P* values less than .05 were considered to be statistically significant in all tests.

RESULTS

The mean and standard deviation of the implant-prosthodontic gap in the x-, y-, and z-axes are represented in Table 3. Significantly lower values were found

Table 1 Process Characteristics of SLS, SLM, and EBM Technologies

	Group		
	SLM-1	SLM-2	SLM-3
Technology manufacturer	SLM Concept Laser	SLM 3D Systems Layerwise-Dentwise	SLM Renishaw
AM metal printer	NA	NA	Renishaw AM250
Co-Cr powder	Remanium star CL	CoCr 3DS	CoCr DG1
Co-Cr powder composition (%)	Co: 60.5 Cr: 28 W: 9 Si: 1.5 Fe, Mn N, Nb and free form Ni, Be, Ga < 1	Co: 59 Cr: 25 W: 9.5 Mo: 3.5 Si: 1 C, Fe, Mn, N: < 1.5	Co: 63.9 Cr: 24.7 Mo: 5 Ni < 0.5 N < 0.25 Fe < 0.5 Mn < 1 Al < 0.10 0 < 0.10 C < 0.05

SLS = selective laser sintering; SLM = selective laser melting; EBM = electron beam melting; AM = additive manufacturing; NA = not available.

Table 2 Mechanical Properties of Co-Cr SLM Additive Manufacturing Processes Provided by Manufacturers

Property	Concept Laser Remanium star CL	3D Systems Dentwise CoCr 3DS	Renishaw CoCr DG1
Alloy type ISO 22674	5	4	4
Density (g/cm^3)	8.6	8.8	8.5
Tensile strength (MPa)	1,030	910	1,097–1,104
Yield strength (MPa)	635	650	683–714
Elongation at break (%)	10	8	16–21
Young's modulus (GPa)	230	200	220
Hardness (HV)	NA	310	400–412
Coefficient thermal expansion (°C)	14.1×10^{-6}/°C	14.0×10^{-6}/°C	10.2×10^{-6}
Melting interval (°C)	1,320–1,420	1,305–1,400	1,260–1,482

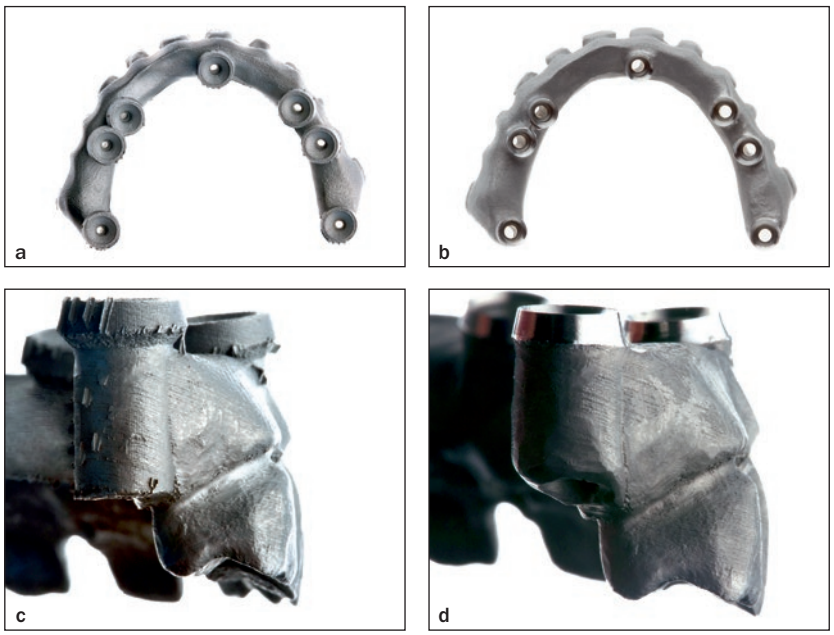

Fig 3 *(a)* Complete-arch Co-Cr implant framework manufactured through SLM technology without the CNC machining of the implant interface. *(b)* Co-Cr implant additive manufacturing framework after the CNC machining of the implant interface. *(c)* Detail of the superficial texture of the 3D printed metal before the machining of the implant interface. *(d)* Detail of the final metal 3D printed framework.

Fig 4 Complete-arch Co-Cr implant framework from *(a)* SLM-1, *(b)* SLM-2, and *(c)* SLM-3 groups.

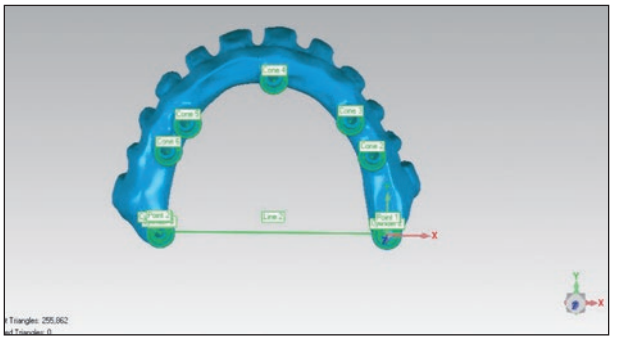

Fig 5 Coordinate measuring machine analysis of a metal framework, with the best-fit technique to measure the implant-prosthodontic gap.

Table 3 Mean, SD, Minimum, Maximum, and Confidence Interval Levels (95%) of Implant-Prosthodontic Discrepancy in x-, y-, and z-axis and 3D Gap Calculations (μm)

						95% CI for mean			
		n	Mean	SD	Standard error	Lower bound	Upper bound	Minimum	Maximum
X-axis	SLM-1	63	34.7737	21.85197	2.75309	40.2770	40.2770	.12	72.17
	SLM-2	63	16.2137	9.60329	1.20990	18.6322	18.6322	3.45	32.04
	SLM-3	63	32.9183	27.76995	3.49868	39.9120	39.9120	2.48	92.32
	Total	189	27.9685	22.63283	1.64630	31.2161	31.2161	.12	92.32
Y-axis	SLM-1	63	54.3481	29.89625	3.76657	61.8774	61.8774	1.24	127.45
	SLM-2	63	38.8392	27.81574	3.50445	45.8445	45.8445	3.67	98.55
	SLM-3	63	27.9679	9.49048	1.19569	30.3581	30.3581	6.23	44.44
	Total	189	40.3851	26.40886	1.92096	44.1745	44.1745	1.24	127.45
Z-axis	SLM-1	63	16.1367	21.09152	2.65728	21.4485	21.4485	.79	80.45
	SLM-2	63	9.0941	7.63184	.96152	11.0162	11.0162	.63	22.94
	SLM-3	63	4.0137	2.29398	.28901	4.5914	4.5914	.04	8.89
	Total	189	9.7481	13.87409	1.00919	11.7389	11.7389	.04	80.45
3D gap	SLM-1	63	73.7706	27.94452	3.52068	80.8084	80.8084	30.98	128.93
	SLM-2	63	47.5365	22.62765	2.85082	53.2352	53.2352	25.31	100.45
	SLM-3	63	47.2567	22.57526	2.84422	52.9422	52.9422	21.28	101.13
	Total	189	56.1879	27.38373	1.99187	60.1172	60.1172	21.28	128.93

at the z-axis, followed by the x- and y-axes (Table 4, Figs 6a to 6d) ($P < .05$). The statistical power was calculated for the x-, y-, and z-axes and 3D gap measurements, with 93.6%, 96.5%, and 72.4% for the x-, y-, and z-axes, respectively, and 91% for the 3D gap.

The mean 3D implant-prosthodontic discrepancy (μm) was higher for SLM-1 (73.77 ± 27.94) than for SLM-2 (47.54 ± 22.63) and SLM-3 (47.26 ± 22.57).

At the x-axis, SLM-2 showed a significantly smaller gap (16.21 ± 9.6) than SLM-3 (32.92 ± 27.77) and SLM-1

Table 4 Mean Implant-Prosthodontic Discrepancy in the x-, y-, and z-axes and 3D Gap

Dependent variable	(I) Group	(J) Group	Mean difference (I-J)	Standard error	*P*
X-axis	SLM-1	SLM-2	18.56000*	3.76689	.000
		SLM-3	1.85540	3.76689	.875
	SLM-2	SLM-1	–18.56000*	3.76689	.000
		SLM-3	–16.70460*	3.76689	.000
	SLM-3	SLM-1	–1.85540	3.76689	.875
		SLM-2	16.70460*	3.76689	.000
Y-axis	SLM-1	SLM-2	15.50889*	4.31261	.001
		SLM-3	26.38016*	4.31261	.000
	SLM-2	SLM-1	–15.50889*	4.31261	.001
		SLM-3	10.87127*	4.31261	.033
	SLM-3	SLM-1	–26.38016*	4.31261	.000
		SLM-2	–10.87127*	4.31261	.033
Z-axis	SLM-1	SLM-2	7.04254*	2.31937	.008
		SLM-3	12.12302*	2.31937	.000
	SLM-2	SLM-1	–7.04254*	2.31937	.008
		SLM-3	5.08048	2.31937	.075
	SLM-3	SLM-1	–12.12302*	2.31937	.000
		SLM-2	–5.08048	2.31937	.075
3D gap	SLM-1	SLM-2	26.23413*	4.36745	.000
		SLM-3	26.51397*	4.36745	.000
	SLM-2	SLM-1	–26.23413*	4.36745	.000
		SLM-3	0.27984	4.36745	.998
	SLM-3	SLM-1	–26.51397*	4.36745	.000
		SLM-2	–0.27984	4.36745	.998

Tukey test; *$P < .05$.

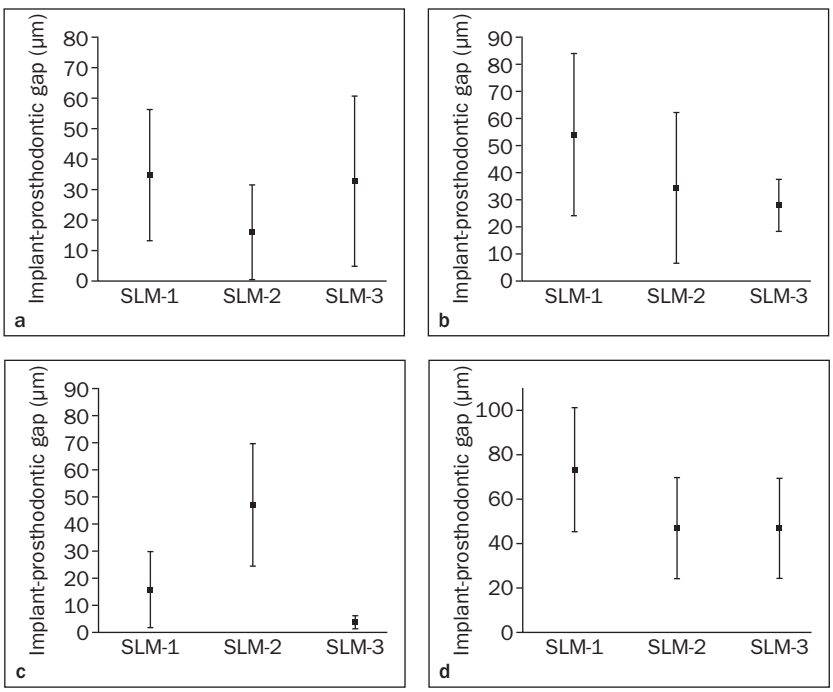

Fig 6 Means and standard deviations of the implant-prosthodontic gap (µm): *(a)* in the x-axis; *(b)* in the y-axis; *(c)* in the z-axis; *(d)* 3D gap calculations for the SLM-1, SLM-2, and SLM-3 groups obtained using a coordinate measuring machine.

Table 5 Means of Implant-Prosthodontic Discrepancy for Three Groups Tested in Homogenous Subsets (alpha = .05) for x-axis

		Subset for alpha = .05	
Groups	**n**	**1**	**2**
Student-Newman-Keuls			
SLM-2	63	16.2137	
SLM-3	63		32.9183
SLM-1	63		34.7737
P		1.000	.623
Tukey HSD			
SLM-2	63	16.2137	
SLM-3	63		32.9183
SLM-1	63		34.7737
P		1.000	.875

Table 6 Means of Implant-Prosthodontic Discrepancy for Three Groups Tested in Homogenous Subsets (alpha = .05) for y-axis

		Subset for alpha = .05		
Groups	**n**	**1**	**2**	**3**
Student-Newman-Keuls				
SLM-2	63	27.9679		
SLM-3	63		38.8392	
SLM-1	63			54.3481
P		1.000	1.000	1.000
Tukey HSD				
SLM-2	63	27.9679		
SLM-3	63		38.8392	
SLM-1	63			54.3481
P		1.000	1.000	1.000

Table 7 Means of Implant-Prosthodontic Discrepancy for Three Groups Tested in Homogenous Subsets (alpha = .05) for z-axis

		Subset for alpha = .05		
Groups	**n**	**1**	**2**	**3**
Student-Newman-Keuls				
SLM-2	63	4.0137		
SLM-3	63		9.0941	
SLM-1	63			16.1367
P		1.000	1.000	1.000
Tukey HSD				
SLM-2	63	4.0137		
SLM-3	63	9.0941		
SLM-1	63		16.1367	
P		.075	1.000	

Table 8 Means of Implant-Prosthodontic Discrepancy for Three Groups Tested in Homogenous Subsets (alpha = .05) for 3D Gap

		Subset for alpha = .05	
Groups	**n**	**1**	**2**
Student-Newman-Keuls			
SLM-2	63	47.2567	
SLM-3	63	47.5365	
SLM-1	63		73.7706
P		.949	1.000
Tukey HSD			
SLM-2	63	47.2567	
SLM-3	63	47.5365	
SLM-1	63		73.7706
P		.998	1.000

(34.77 ± 21.85). At the y-axis, however, SLM-3 presented a significantly smaller gap (27.97 ± 9.49) than those of SLM-2 (38.84 ± 27.82) and SLM-1 (54.35 ± 29.89) (Tables 5 to 8). Similarly, at the z-axis, SLM-3 showed the least gap (4.01 ± 2.29) followed by SLM-2 (9.09 ± 7.63), which was significantly smaller than that of SLM-1 (16.14 ± 21.09).

DISCUSSION

Additive manufacturing technologies combined with the CNC machining of the implant interface is a viable option when manufacturing the metal framework of an implant-supported dental prosthesis. However, the implant-prosthodontic discrepancy that additive and subtractive technologies combined can obtain is unclear. In the present study, statistically significant differences were found between the different SLM additive manufacturing metal frameworks on the implant-prosthodontic discrepancy in the x-, y-, and z-axis and 3D gap measurements; therefore, the null hypothesis was rejected.

In the present study, the 3D gap measurements of the complete-arch Co-Cr SLM additive manufacturing implant frameworks ranged between 47.26 ± 22.57 µm

and 73.77 ± 27.94 µm, which can be considered acceptable for clinical use.[42] Riedy et al[51] reported that the smallest gap that can be detected by the human eye is from 50 to 100 µm. Hence, the implant-prosthodontic discrepancy encountered in the present study could not be detected clearly by the human eye on the direct vision evaluation.

Additive manufacturing technologies offer several advantages compared with the conventional casting method, namely, highly reduced manufacturing time and costs, product density, prevention of casting defects applied for metal alloys, and minimization of human intervention.[9,10] However, SLM technology is based on a layer-by-layer building-up process that results in a characteristic superficial texture in the 3D printed metal.[8–11] Therefore, the CNC machining is required to mill the implant interface, providing a smooth surface and obtaining the precision for an adequate implant-prosthodontic gap.

Fernández et al[42] quantified the roughness of the mating surfaces of implant components fabricated with different processes, namely, cast, milled, and additive manufacturing, and measured the microgap between implant components using scanning electron microscopy (SEM) analysis. In addition, correlation between microroughness and the microgap was investigated. The mean roughness values reported were 29, 115, and 98 mm for cast, milled, and additive manufacturing, respectively. Implant-prosthodontic discrepancy for the single-unit abutment was 0.73, 9.09, and 11.30 mm for cast, milled, and additive manufacturing groups, respectively. However, it was unclear whether the additive manufacturing group combined with the CNC technology could reduce the superficial roughness of the 3D printed metal, which may affect the outcome of the study. Also, a single-unit metal framework, compared with a complete-arch framework supported by seven implants, represents an easier and more predictable clinical situation to obtain a smaller implant-prosthodontic discrepancy, whereas multiple implants and deviations in positions represent numerous variances in depth and angulation between the different implants present in the patient's mouth. These aspects were not involved in this study, which could be considered as a limitation of this study.

In another study, Revilla-León et al[33] reported discrepancies of complete-arch titanium (Ti6Al4V) frameworks supported by four implants and manufactured using SLM and EBM additive manufacturing technologies where the implant-prosthodontic discrepancy of the frameworks was measured in the x-, y-, and z-axes through a CMM. The same STL file was used to manufacture all the specimens. Except for the z-axis, no significant differences were observed between the SLM and EBM technologies for implant-prosthesis discrepancy for the x- or y-axes. The mean 3D discrepancy was 6 ± 13.5 mm for the SLM technology and 60.2 ± 18.5 mm for the EBM technology. Indeed, the highest discrepancy was observed in the y-axis (37 to 56 mm), followed by the x- (16 to 44 mm) and z- (6 to 11 mm) axes, which are considered to be clinically acceptable. The 3D gap values measured in the present study are in similar ranges. However, statistical differences were found on the x-, y-, and z-axes, which could be explained by the different metal processed, different additive manufacturing selected, and/or different CNC used to mill the implant interface.

Previous studies have reported a lower discrepancy on the z-axis compared with the x- and y-axes, which is in agreement with the results of the present study.[49–56] Moreover, the vertical fit of Co-Cr CAD/CAM frameworks seems to be smaller than that of Co-Cr frameworks fabricated by casting procedures.[55,56] Based on the current literature, the acceptable level of the vertical misfit (z-axis) varies from 30 to 150 µm; however, no agreement is currently available.[31–40] Even though statistically significant discrepancies were found between the groups, the mean vertical gap of the Co-Cr SLM frameworks ranged between 4.01 ± 2.29 µm and 16.14 ± 21.09 µm.

Currently, diverse methods are available to assess precision of fit.[42–46,57] The best-fit technique is the least square method that is based on measurements using a "virtual" approach where the finest fitting possible is simulated on the computer. Nevertheless, in clinical practice, the physical components would have prevented such low levels of distortion. Consequently, vertical discrepancy is undervalued by using these analysis methods, and interpretations in the clinic should be approached with much caution.[42–46]

CONCLUSIONS

The three SLM additive manufacturing technologies tested for manufacturing complete-arch Co-Cr implant-supported frameworks obtained an implant-prosthodontic discrepancy ranging between 4.01 ± 2.29 and 54.35 ± 29.9 µm, which could be considered in the clinically acceptable range. Overall, the z-axis showed less distortion compared with the x- and y-axes in all the groups evaluated.

ACKNOWLEDGMENTS

The authors declare no conflicts of interest.

REFERENCES

1. Singh V. Rapid prototyping, materials for RP and applications of RP. Int J Eng Res Sci 2013;4:473–480.
2. Al-Jubouri O, Azzari A. An introduction to dental digitizers in dentistry: Systematic review. J Chem Pharm Res 2015;7:10–20.
3. Tapie L, Lebon N, Mawussi B, Fron-Chabouis H, Duret F, Attal JP. Understanding dental CAD/CAM for restorations—accuracy from a mechanical engineering viewpoint. Int J Comput Dent 2015;18:343–367.
4. Rudolph H, Luthardt RG, Walter MH. Computer-aided analysis of the influence of digitizing and surfacing on the accuracy in dental CAD/CAM technology. Comput Biol Med 2007;37: 579–587.
5. Stereo Lithography Interface Specification. 3D Systems: Valencia, California, 1988.
6. ASTM, Committee F42 on Additive Manufacturing Technologies, West Conshohocken, Pennsylvania. 2009 Standard Terminology for Additive Manufacturing – General Principles and Terminology. ISO/ASTM52900-15.
7. Witkowski S. CAD-/CAM in dental technology. Quintessence Dent Technol 2005;28:169–184.
8. Vandenbroucke B, Kruth JP. Selective laser melting of biocompatible metals for rapid manufacturing of medical parts. Rapid Prototyp J 2007;13:196–203.
9. Horn TJ, Harrysson OLA. Overview of current additive manufacturing technologies and selected applications. Sci Prog 2012;95:255–282.
10. Revilla-León M, Özcan M. Additive Manufacturing Technologies Used for 3D Metal Printing in Dentistry. Curr Oral Health Rep 2017;4:201–208.
11. Deckard CR. 1986. Patent US 4863538-A. Method and apparatus for producing parts by selective sintering.
12. Deckard C, Beaman JJ. Process and control issues in selective laser sintering. ASME Prod Eng Div 1988;33:191–197.
13. Fisher P, Karapatis N, Romano V, Glardon R, Weber HP. A model for the interaction of near-infrared laser pulses with metal powders in selective laser sintering. Appl Phys A 2002;74:467–474.
14. Örtop A, Jönsson D, Mouhsen A, Vult von Steyern P. The fit of cobalt-chromium three-unit fixed dental prostheses fabricated with four different techniques: A comparative in vitro study. Dent Mater 2011;27:356–363.
15. Goodridge RD, Tuck CJ, Hague RJ. Laser sintering of polyamides and other polymers. Progr Mater Sci 2012;57:229–267.
16. Suleiman SH, Vult von Steyern P. Fracture strength of porcelain fused to metal crowns made of cast, milled or laser-sintered cobalt-chromium. Acta Odontol Scand 2013;71:1280–1289.
17. Kim KB, Kim JH, Kim WC, Kim JH. Three-dimensional evaluation of gaps associated with fixed dental prostheses fabricated with new technologies. J Prosthet Dent 2014;112:1432–1436.
18. Tamac E, Toksavul S, Toman M. Clinical marginal and internal adaptation of CAD/CAM milling, laser sintering and cast metal ceramic crowns. J Prosthet Dent 2014;112:909–913.
19. Osakada K, Shiomi M. Flexible manufacturing of metallic products by selective laser melting of powder. Int J Mach Tool Manu 2006;46:1188–1193.
20. Murr LE, Martinez E, Gaytan SM, et al. Microstructural architecture, microstructures, and mechanical properties for a nickel-base superalloy fabricated by electron beam melting. Metall Mater Trans A 2011;42:3491–3508.
21. Murr LE, Gaytan SM, Ramirez DA, et al. Metal fabrication by additive manufacturing using laser and electron beam melting technologies. J Mater Sci Technol 2012;28:1–14.
22. Yadroitsev I, Krakhmalev P, Yadroitsava I, Johansson S, Smurov I. Energy input effect on morphology and microstructure of selective laser melting single track from metallic powder. J Mater Process Technol 2013;213:606–613.
23. Petrovic V, Haro JV, Blasco JR, Portolés L. Additive manufacturing solutions for improved medical implants. Biomedicine, Dr. Chao Lin (ed). InTech.
24. Frazier WE. Metal additive manufacturing: A review. J Mater Eng Perform 2014;23:1917–1928.
25. Qian B, Saeidi K, Kvetková L, Lofaj F, Xiao C, Shen Z. Defects-tolerant Co-Cr-Mo dental alloys prepared by selective laser melting. Dent Mater 2015;31:1435–1444.
26. Parthasarathy J, Starly B, Raman S, Christensen A. Mechanical evaluation of porous titanium (Ti6Al4V) structures with electron beam melting (EBM). J Mech Behav Biomed Mater 2010;3:249–259.
27. Petrović V, Blasco JR, Portolés L, et al. A study of mechanical and biological behavior of porous Ti6Al4V fabricated on EBM. Innovative developments in virtual and physical prototyping – proceedings. VRAP 2012;28:115–120.
28. Karpuschewski B, Pieper HJ, Krause M. Co-Cr is not the same: CrCo-blanks for dental machining. In: Schuh G. Neugebauer R, Uhlmann E (eds). Future Trends in Production Engineering. Berlin: Springer-Verlag, 2013:261–274.
29. Takaichi A, Suyalatu, Nakamoto T, et al. Microstructures and mechanical properties of Co-29Cr-6Mo alloy fabricated by selective laser melting process for dental applications. J Mech Behav Biomed Mater 2013;21:67–76.
30. Al Jabbari YS, Koutsoukis T, Barmpagadaki X, Zinelis S. Metallurgical and interfacial characterization of PFM Co-Cr dental alloys fabricated via casting, milling or selective laser melting. Dent Mater 2014;30:e79–e88.
31. Koutsoukis T, Zinelis S, Eliades G, Al-Wazzan K, Al Rifaiy M, Al Jabbari YS. Selective laser melting technique of Co-Cr dental alloys: A review of structure and properties and comparative analysis with other available techniques. J Prosthodont 2015;24:303–312.
32. Gelbard S, Aoskar Y, Zalkind M, Stern N. Effect of impression materials and techniques on the marginal fit of metal castings. J Prosthet Dent 1994;71:1–6.
33. Revilla-León M, Ceballos L, Martínez-Klemm I, Özcan M. Discrepancy of complete-arch titanium frameworks manufactured using selective laser melting and electron beam melting additive manufacturing technologies. J Prosthet Dent 2018;120:942–947.
34. Willis LM, Nicholls JI. Distortion in dental soldering as affected by gap distance. J Prosthet Dent 1980;43:272–278.
35. Ziebert GJ, Hurtado A, Glapa C, Schiffleger BE. Accuracy of one-piece castings, preceramic and postceramic soldering. J Prosthet Dent 1986;55:312–317.
36. Tan KB, Rubenstein JE, Nicholls JI, Youdelis RA. Three-dimensional analysis of the casting accuracy of one-piece, osseointegrated implant-retained prostheses. Int J Prosthodont 1993;6:346–363.
37. Goll GE. Production of accurately fitting full-arch implant frameworks: Part I—clinical procedures. J Prosthet Dent 1991;66:377–384.
38. Carr AB, Brunski JB. Preload and load sharing of strain gauged CP-Ti implant components. J Dent Res 1992;71:528.
39. Binon PP. Evaluation of machining accuracy and consistency of selected implants, standard abutments, and laboratory analogs. Int J Prosthodont 1995;8:162–178.
40. Jemt T, Lie A. Accuracy of implant-supported prostheses in the edentulous jaw: Analysis of precision of fit between cast gold-alloy framework and master cast by means of three-dimensional photogrammetric technique. Clin Oral Implants Res 1995;6:172–180.
41. Kan JY, Rungcharassaeng K, Bohsalu K, Goodacre CJ, Lang BR. Clinical methods for evaluating implant framework fit. J Prosthet Dent 1999;81:7–13.
42. Fernández M, Delgado L, Molmeneu M, García D, Rodríguez D. Analysis of the misfit of dental implant-supported prostheses made with three manufacturing processes. J Prosthet Dent 2014;111:116–123.
43. Jemt T. Failures and complications in 391 consecutively inserted fixed prostheses supported by Brånemark implant in the edentulous jaws: A study of treatment from the time of prosthesis placement to the first annual check-up. Int J Oral Maxillofac Implants 1991;6:270–276.
44. Jemt T. Three-dimensional distortion of gold alloy castings and welded titanium frameworks. Measurements of the precision of fit between completed implant prostheses and the master casts in routine edentulous situations. J Oral Rehabil 1995;22:557–564.
45. Jemt T, Rubenstein JE, Carlsson L, Lang BR. Measuring fit at the implant prosthodontic interface. J Prosthet Dent 1996;75:314–325.
46. Örtorp A, Jemt T, Bäck T, Jälevik T. Comparisons of precision of fit between cast and CNC-milled titanium implant frameworks for the edentulous mandible. Int J Prosthodont 2003;16:194–200.

47. Observational errors and the calculation of probabilities. In: Hall T (ed). Carl Friedrich Gauss: A Biography. Cambridge, Massachusetts: MIT Press, 1970:74–78.
48. Buhler WE. Gauss, A Biographical study. The method of least squares. Berlin: Springer-Verlag, 1981:138–141.
49. Klineberg IJ, Murray GM. Design of superstructures for osseointegrated fixtures. Swed Dent J Suppl 1985;28:63–69.
50. Cheshire PD, Hobkirk JA. An in vivo quantitative analysis of the fit of Nobel Biocare implant superstructures. J Oral Rehabil 1996;23:782–789.
51. Riedy SJ, Lang BR, Lang BE. Fit of implant framework fabricated by different techniques. J Prosthet Dent 1997;78:596–604.
52. Takahashi T, Gunne J. Fit of implant frameworks: An in vitro comparison between two fabrication techniques. J Prosthet Dent 2003;89:256–260.
53. Al-Fadda SA, Zarb GA, Finer Y. A comparison of the accuracy of fit of 2 methods for fabricating implant-prosthodontic frameworks. Int J Prosthodont 2007;20:125–131.
54. Eliasson A, Wenneberg A, Johansson A, Örtorp A, Jemt T. The precision of the fit of milled titanium implant frameworks (I-Bridge) in the edentulous jaw. Clin Implant Dent Relat Res 2010;12:81–90.
55. Hjalmarsson L, Örtorp A, Smedberg JI, Jemt T. Precision of fit to implants: A comparison of Cresco and Procera implant bridge frameworks. Clin Implant Dent Relat Res 2010;12:271–280.
56. De Torres EM, Barbosa GA, Bernardes SR, de Mattos Mda G, Ribeiro RF. Correlation between vertical misfits and stresses transmitted to implants from metal frameworks. J Biomech 2011;44:1735–1739.
57. Eliasson A, Wennerberg A, Johansson A, Örtop A, Jemt T. The precision of fit of milled titanium implant frameworks (I-Bridge) in the edentulous jaw. Clin Implant Dent Relat Res 2010;12:81–90.